

# Constraints on WIMP Dark Matter from the High Energy PAMELA $\bar{p}/p$ data

F. Donato

*Dipartimento di Fisica Teorica, Università di Torino  
Istituto Nazionale di Fisica Nucleare, via P. Giuria 1, I-10125 Torino, Italy*

D. Maurin

*Laboratoire de Physique Nucléaire et Hautes Energies, CNRS-IN2P3/Université Paris VII,  
4 Place Jussieu, Tour 33, 75252 Paris Cedex 05, France*

P. Brun

*CEA, Irfu, Service de Physique des Particules, Centre de Saclay, F-91191 Gif-sur-Yvette, France*

T. Delahaye and P. Salati

*Laboratoire d'Annecy-le-Vieux de Physique Théorique LAPTH, CNRS  
and Université de Savoie 9, Chemin de Bellevue, B.P.110 74941 Annecy-le-Vieux, France*

(Dated: October 29, 2008)

A new calculation of the  $\bar{p}/p$  ratio in cosmic rays is compared to the recent PAMELA data. The good match up to 100 GeV allows to set constraints on exotic contributions from thermal WIMP dark matter candidates. We derive stringent limits on possible enhancements of the WIMP  $\bar{p}$  flux: a  $m_{\text{WIMP}}=100$  GeV (1 TeV) signal cannot be increased by more than a factor 6 (40) without overrunning PAMELA data. Annihilation through the  $W^+W^-$  channel is also inspected and cross-checked with  $e^+/(e^- + e^+)$  data. This scenario is strongly disfavored as it fails to simultaneously reproduce positron and antiproton measurements.

PACS numbers: L1

The cosmic ray (CR) antiproton and positron fluxes are considered as prime targets for indirect detection of galactic dark matter (DM). A deviation from the predicted astrophysical background has been searched for mostly at low energy (e.g., [1]). However, in some scenario, heavy Weakly Interacting Massive Particle (WIMP) candidates—either from annihilation of the lightest supersymmetric species, or from the lightest Kaluza-Klein particles in universal extra dimensions—should be able to provide sizeable fluxes beyond a few GeV [2]. The PAMELA collaboration has recently published the cosmic ray antiproton to proton ratio in the hitherto unexplored  $\sim 1 - 100$  GeV energy range [3]. We find that the background flux, yielded by standard astrophysical processes, can explain the data up to high energies. Adding a contribution from the annihilation of a generic WIMP dark matter halo, we derive stringent upper limits on possible boost factors of the exotic  $\bar{p}$  flux. In addition, in some scenarios, the WIMPs mostly annihilate into  $W^+W^-$  pairs, hence giving rise to a copious amount of hard positrons. Recent calculations, in the light of the new PAMELA measurement of the positronic fraction in CRs, showed that the secondary production alone could explain the data [4]. Would an heavy WIMP be required to better match the positron flux, we also

check the viability of such models through the combined constraints from the  $e^+$  and  $\bar{p}$  fluxes.

The secondary  $\bar{p}$  flux provided in this paper is an improved calculation of that presented in [18], to which we refer for a thorough discussion of the ingredients and the technical details. Antiprotons are yielded by the spallation of cosmic ray proton and helium nuclei over the interstellar medium, the contribution of heavier nuclei being negligible [19]. Even if only p and He with kinetic energy larger than  $6 m_p$  can produce  $\bar{p}$ , a good description of the p and He interstellar (IS) fluxes is mandatory to correctly provide the  $\bar{p}/p$  ratio in the 0.1 GeV–100 GeV range. Following [20], we model the proton and helium IS fluxes as

$$\Phi = A\beta^{P_1} R^{-P_2} \text{ m}^{-2} \text{ s}^{-1} \text{ sr}^{-1} (\text{GeV/n})^{-1}, \quad (1)$$

where  $R$  is the rigidity of the particle. The parameterization for the fluxes below 20 GeV/n are taken from the reanalysis of the 1997 to 2002 BESS data [20]:  $\{A, P_1, P_2\} = \{19400, 0.7, 2.76\}$  for H and  $\{7100, 0.5, 2.78\}$  for He. For the high energy range, the combined fit of AMS-01 [21–23], BESS98 [24] and BESS-TeV [25] demodulated data respectively give  $\{A, P_1, P_2\} = \{24132, 0., 2.84\}$  for H and  $\{8866, 0., 2.85\}$  for He. The two fits connect smoothly at 20 GeV/n. Compared to [18], we also improve the

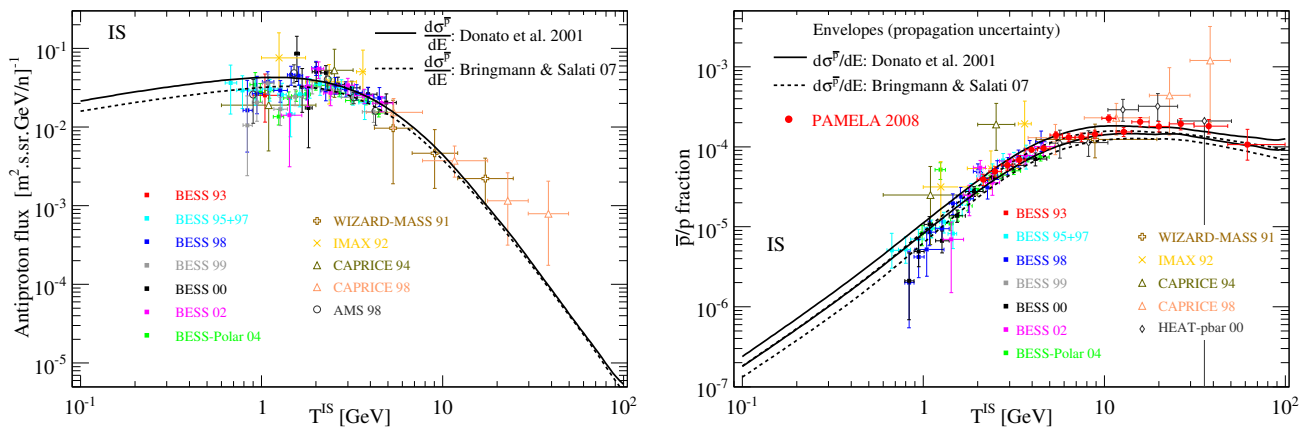


FIG. 1: Left panel: IS antiproton flux for the B/C best fit model and two parameterizations of the production cross section. Right panel: propagation uncertainty envelopes of the IS  $\bar{p}/p$  ratio for the same production cross sections as in the left panel. All data are demodulated using the force-field approximation: AMS 98 [5], IMAX 92 [6], CAPRICE 94 [7], WIZARD-MASS 91 [8], CAPRICE 98 [9], BESS93 [10], BESS 95+97 [11], BESS 98 [12], BESS 99 and 2000 [13], BESS 2002 [14], BESS Polar [15], WIZARD-MASS 1 [16], HEAT- $\bar{p}$  [17], and PAMELA [3].

calculation of the tertiary mechanism [26]. The Anderson prescription [27] is used, as described in [19, 28]. As a result, the low energy tail is more replenished, leading to a larger flux. The framework used to calculate cosmic ray fluxes is the diffusion model with convection and reacceleration. The transport parameters are fixed from the boron-to-carbon (B/C) analysis [29] and correspond to i) the diffusion halo of the Galaxy  $L$ ; ii) the normalization of the diffusion coefficient  $K_0$  and its slope  $\delta$  ( $K(E) = K_0 \beta R^\delta$ ); iii) the velocity of the constant wind directed perpendicular to the galactic disk  $\vec{V}_c = \pm V_c \vec{e}_z$ ; and iv) the reacceleration strength mediated via the Alfvénic speed  $V_a$ . Strong degeneracies are observed among the allowed parameter sets [29], but it has a limited impact on the secondary  $\bar{p}$  flux [18]. At variance, the corresponding DM-induced  $\bar{p}$  flux suffers large propagation uncertainties [30]; this is also the case for the secondary and primary positron fluxes [4, 31]. Throughout the paper, the fluxes will be shown for the B/C best fit propagation parameters, i.e.  $L = 4$  kpc,  $K_0 = 0.0112$  kpc<sup>2</sup>Myr<sup>-1</sup>,  $\delta = 0.7$ ,  $V_c = 12$  km s<sup>-1</sup> and  $V_a = 52.9$  km s<sup>-1</sup> [29].

The secondary IS  $\bar{p}$  flux is displayed in the left panel of Fig. 1 along with the data demodulated according to the force-field prescription. We either use the DTUNUC [18]  $\bar{p}$  production cross sections (solid line) or those discussed in [2, 19] (dashed line). The differences between the two curves illustrate the uncertainty related to the production cross sections, as emphasized in [18], where a careful and conservative analysis within the DTUNUC simulation settled a nuclear uncertainty of  $\sim 25\%$  over

the energy range 0.1 – 100 GeV. The conclusion is similar here, although the two sets of cross sections differ mostly at low energy. In the right panel, along with the demodulated  $\bar{p}/p$  data, we show the curves bounding the propagation uncertainty on the  $\bar{p}$  calculation based either on the DTUNUC [18]  $\bar{p}$  production cross sections (solid lines) or those borrowed from [2] (dashed lines). The uncertainty arising from propagation is comparable to the nuclear one [18]. From a bare eye inspection, it is evident that the secondary contribution alone explains PAMELA data on the whole energetic range. It is not necessary to invoke an additional component to the standard astrophysical one.

Motivated by the accuracy of our predictions and their well understood theoretical uncertainties, as well as by the good statistical significance of PAMELA data, we derive limits on a possible exotic component. We focus on the high energy part of the  $\bar{p}/p$  ratio, where solar modulation does not play any role [32]. We assume an additional component of antiprotons produced by annihilation of WIMPs filling the dark halo of the Milky Way. Their distribution is taken as a cored-isothermal sphere with local density  $\rho_\odot = 0.3$  GeV cm<sup>-3</sup>. The velocity-averaged annihilation cross section is taken as  $\langle \sigma_{\text{ann}} v \rangle = 3 \times 10^{-26}$  cm<sup>3</sup>s<sup>-1</sup>, with an annihilation channel into  $b\bar{b}$ . According to [30], the propagated primary  $\bar{p}$  flux is only very mildly dependent on the annihilation channel and the DM distribution function. Therefore, our assumptions can be considered valid for a generic WIMP dark matter candidate except for a rough rescaling factor. Propagation is treated in the same way as for the secondary compo-

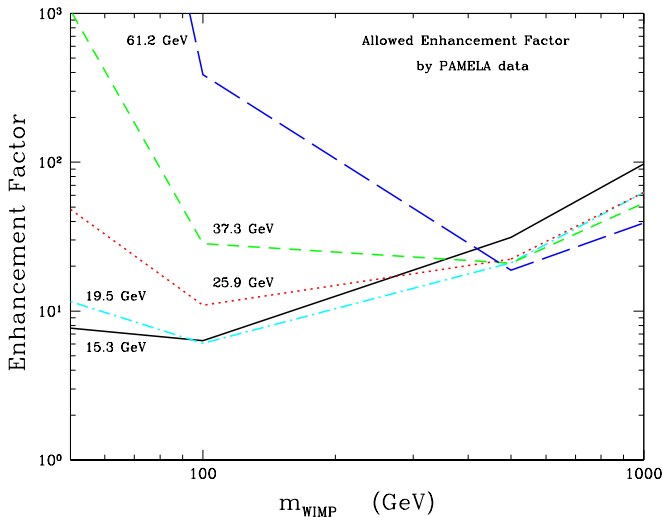


FIG. 2: Upper limits on the enhancement factor to the primary  $\bar{p}$  flux as a function of the WIMP mass, derived from a comparison with PAMELA high energy data. Each curve is labelled according to the corresponding PAMELA energy bin.

ment [28, 30]. As a reference case, we employ the best fit transport parameters listed above and recall that the uncertainty on the primary  $\bar{p}$  flux due to propagation spans roughly one order of magnitude above and one below the best fit scenario. We add the calculated primary  $\bar{p}$  flux for different WIMP masses to the secondary component and compare the total flux to PAMELA high energy data, namely  $T_{\bar{p}} > 10$  GeV. To be conservative, the background calculated from Bringmann & Salati’s  $\bar{p}$  production cross sections is considered (dashed curves in Fig. 1). We derive the factor one could enhance the DM flux without exceeding experimental data ( $2\sigma$  error bars) in any energy bin. The maximum allowed enhancement factor is plotted in Fig. 2 as a function of the WIMP mass: it cannot exceed 6–20–40 for  $m_{\text{WIMP}}=100$ –500–1000 GeV, respectively. These limits can be reinforced as well as relaxed by quite simple modifications of the key ingredients in the flux calculation, just as described above. The boost factor may be ascribed, in principle, to clumpiness in the DM distribution [33]—this contribution being energy-dependent—as well as to an increase of the annihilation cross section as proposed by [34] and more recently by [35] as regards the Sommerfeld effect.

Our conclusions have important consequences on the explanations of the positron data based on the annihilation of DM species within the Milky Way halo. The positron fraction suffers from large uncertainties related for instance to the poorly determined electron spectral index above 10 GeV [4]. Although soft electrons are as-

sociated to large values of the positron fraction and to an agreement of the pure secondary positron flux with the measurements, we cannot dismiss the possibility of a hard cosmic ray electron distribution. A spectral index of 3.44 leads actually in the left panel of Fig. 3 to the long-dashed curve featuring a low background case. With a typical annihilation cross section  $\langle\sigma_{\text{ann}}v\rangle$  of  $3 \times 10^{-26} \text{ cm}^3\text{s}^{-1}$ , WIMPs do not produce enough positrons to reproduce the increasing trend observed in  $e^+/(e^++e^-)$  data [39], so that a significant enhancement of the annihilation rate is necessary as shown in [40]. However the boost factor associated to DM clumps cannot exceed at most a factor of  $\sim 10$  in the standard  $\Lambda$ -CDM scenario of structure formation [33]. Astrophysics does not provide then a natural explanation for the large boost factors required to fit the positron excess. That is why the Sommerfeld effect [35] has been advocated as a plausible mechanism to significantly increase the WIMP annihilation cross section in the non-relativistic regime prevailing today in galactic haloes. Heavy DM species is a prerequisite. We then consider a generic 1 TeV particle annihilating into  $W^+W^-$  pairs and boost  $\langle\sigma_{\text{ann}}v\rangle$  by a factor of 400 in order to get the solid line in the left panel of Fig. 3. Although an annihilation cross section of  $1.2 \times 10^{-23} \text{ cm}^3\text{s}^{-1}$  is possible should non-perturbative effects be at stake, the consequences on antiprotons are drastic. The red solid curve in the right panel of Fig. 3 features an unacceptable distortion of the  $\bar{p}$  spectrum. The DM positron signal cannot be enhanced without playing havoc with the  $\bar{p}$  measurements.

Nonetheless, notice that ways out are possible whose careful investigation is beyond the scope of this Letter. The value of 400 assumed for the positron signal of Fig. 3 could arise from the combined effects of DM clumpiness and  $\langle\sigma_{\text{ann}}v\rangle$  enhancement. If a generous factor of 10 is assumed for the former—a marginally acceptable value [33]—the latter does not exceed 40. Unlike positrons which are produced locally, the antiprotons detected at the Earth originate from a large region of the Milky Way halo over which substructures may not be as important as in our vicinity. The  $\bar{p}$  flux may not be much enhanced by the presence of DM clumps so that a value of 40 would apply in that case to the antiproton boost. The corresponding blue long-dashed line in the right panel of Fig. 3 features a fairly acceptable  $\bar{p}$  spectrum. Notice also that the cosmic ray propagation model could be different from the one selected here. Once again, positron and antiproton fluxes have different behaviors toward a change in the propagation parameters. For example, the primary  $\bar{p}$  flux could be easily decreased by an order of magnitude without violating B/C data, allowing a Som-

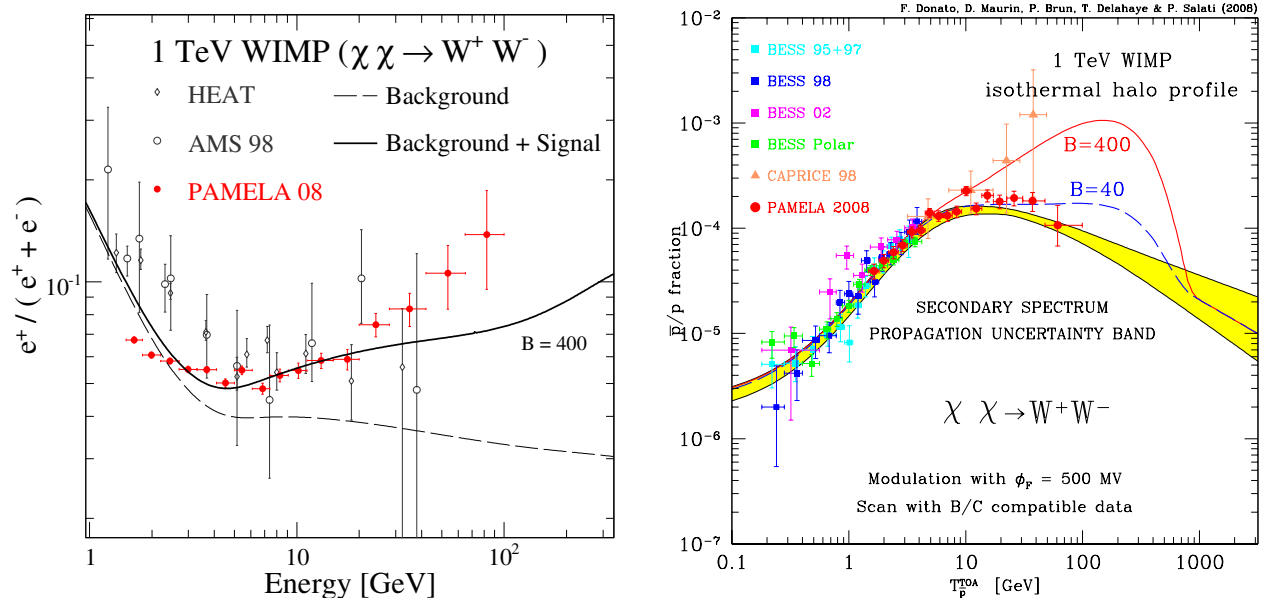


FIG. 3: The fiducial case of a 1 TeV LSP annihilating into a  $W^+W^-$  pair is featured. In the left panel, the positron signal which this DM species yields has been increased by a factor of 400, hence the solid curve and a marginal agreement with the PAMELA data. Positron fraction data are from HEAT [36], AMS-01 [37, 38] and PAMELA [39]. If the so-called Sommerfeld effect [35] is invoked to explain such a large enhancement of the annihilation cross section, the same boost applies to antiprotons and leads to an unacceptable distortion of their spectrum as indicated by the red solid line of the right panel.

merfeld boost of the cross section of 400.

A new calculation for the secondary cosmic antiproton flux and the relevant uncertainties have been presented. The ratio  $\bar{p}/p$  has been derived after fitting recent proton data. Our predictions can explain the experimental data, and in particular the recent PAMELA data, which span more than two decades in energy. No exotic contribution—as from annihilating dark matter in the galactic halo—has to be invoked to reproduce experimental results. Analyzing the high energy part of the PAMELA  $\bar{p}/p$  we derive strong upper limits on possible enhancements of the exotic  $\bar{p}$  flux as a function of the WIMP mass. Relying on standard assumptions the exotic antiproton flux induced by a  $m_{\text{WIMP}} = 100$  GeV (1 TeV) DM halo cannot be increased by more than a factor 6 (40) without overrunning PAMELA data. Would the Sommerfeld effect ( $W^+W^-$  channel) be invoked to explain PAMELA leptonic data, the corresponding enhancement of the  $\bar{p}$  production would lead to an unacceptable distortion of the  $\bar{p}/p$  spectrum.

*Acknowledgements.* F.D. thanks N. Fornengo and M. Boezio for useful discussions. We acknowledge the support from the French Programme National de Cosmologie and the Explora'doc PhD student program.

- [1] A. Bottino, F. Donato, N. Fornengo, and P. Salati, Phys. Rev. D **58**, 123503 (1998).
- [2] T. Bringmann and P. Salati, Phys. Rev. D **75**, 083006 (2007).
- [3] O. Adriani et al. (PAMELA), subm. Phys. Rev. Lett. (2008), 0810.4994.
- [4] T. Delahaye et al., A&A submitted (2008), 0809.5268.
- [5] M. Aguilar et al. (AMS), Phys. Rep. **366**, 331 (2002).
- [6] J. W. Mitchell et al. (IMAX), Phys. Rev. Lett. **76**, 3057 (1996).
- [7] M. Boezio et al. (CAPRICE), ApJ **487**, 415 (1997).
- [8] G. Basini et al. (WIZARD-MASS), ICRC **3**, 77 (1999).
- [9] M. Boezio et al. (CAPRICE), ApJ **561**, 787 (2001).
- [10] A. Moiseev et al. (BESS), ApJ **474**, 479 (1997).
- [11] S. Orito et al. (BESS), Phys. Rev. Lett. **84**, 1078 (2000).
- [12] T. Maeno et al. (BESS), Astropart. Phys. **16**, 121 (2001).
- [13] Y. Asaoka et al. (BESS), Phys. Rev. Lett. **88**, 051101 (2002).
- [14] S. Haino et al. (BESS), ICRC **3**, 13 (2005).
- [15] K. Abe et al. (BESS), ArXiv e-prints (2008), 0805.1754.
- [16] M. Hof et al. (WIZARD-MASS 1), ApJ **467**, L33 (1996).
- [17] A. S. Beach et al. (HEAT), Phys. Rev. Lett. **87**, 271101 (2001).
- [18] F. Donato, D. Maurin, P. Salati, A. Barrau, G. Boudoul, and R. Taillet, ApJ **563**, 172 (2001).
- [19] R. Duperray et al., Phys. Rev. D **71**, 083013 (2005).

- [20] Y. Shikaze et al. (BESS), *Astropart. Phys.* **28**, 154 (2007).
- [21] J. Alcaraz et al. (AMS), *Phys. Lett. B* **490**, 27 (2000).
- [22] J. Alcaraz et al. (AMS), *Phys. Lett. B* **472**, 215 (2000).
- [23] J. Alcaraz et al. (AMS), *Phys. Lett. B* **494**, 193 (2000).
- [24] T. Sanuki et al. (BESS), *ApJ* **545**, 1135 (2000).
- [25] S. Haino et al. (BESS), *Phys. Lett. B* **594**, 35 (2004).
- [26] L. Bergström, J. Edsjö, and P. Ullio, *ApJ* **526**, 215 (1999).
- [27] E. W. Anderson et al., *Phys. Rev. Lett.* **19**, 198 (1967).
- [28] F. Donato, N. Fornengo, and D. Maurin, *Phys. Rev. D* **78**, 043506 (2008).
- [29] D. Maurin, F. Donato, R. Taillet, and P. Salati, *ApJ* **555**, 585 (2001).
- [30] F. Donato, N. Fornengo, D. Maurin, P. Salati, and R. Taillet, *Phys. Rev. D* **69**, 063501 (2004).
- [31] T. Delahaye, R. Lineros, F. Donato, N. Fornengo, and P. Salati, *Phys. Rev. D* **77**, 063527 (2008), 0712.2312.
- [32] J. W. Bieber et al., *Phys. Rev. Lett.* **83**, 674 (1999).
- [33] J. Lavalle, Q. Yuan, D. Maurin, and X.-J. Bi, *A&A* **479**, 427 (2008), 0709.3634.
- [34] L. Bergström, *Physics Letters B* **225**, 372 (1989).
- [35] J. Hisano, S. Matsumoto, and M. M. Nojiri, *Phys. Rev. Lett.* **92**, 031303 (2004).
- [36] S. W. Barwick et al. (HEAT), *ApJ* **482**, L191+ (1997), astro-ph/9703192.
- [37] M. Aguilar et al. (AMS-01), *Phys. Lett.* **B646**, 145 (2007), astro-ph/0703154.
- [38] J. Alcaraz et al. (AMS), *Phys. Lett.* **B484**, 10 (2000).
- [39] O. Adriani et al. (PAMELA) (2008), 0810.4995.
- [40] L. Bergstrom, T. Bringmann, and J. Edsjo (2008), 0808.3725.